

Electronic Energy Distribution Function at High Electron Swarm Energies in Neon*

K. L. Brown and J. Fletcher

School of Physical Sciences, Flinders University,
GPO Box 2100, Adelaide, SA 5001, Australia.

Abstract

Electron swarms moving through a gas under the influence of an applied electric field have been extensively investigated. Swarms at high energies, as measured by the ratio of the applied field to the gas number density, E/N , which are predominant in many applications have, in general, been neglected. Discharges at E/N in the range $300 < E/N < 2500$ Td have been investigated in neon gas in the pressure range $6 < p_0 < 133$ Pa using a differentially pumped vacuum system in which the swarm electrons are extracted from the discharge and energy analysed in both a parallel plate retarded potential analyser and a cylindrical electrostatic analyser. Both pre-breakdown and post-breakdown discharges have been studied. Initial results indicate that as the discharge traverses breakdown no sudden change in the nature of the discharge occurs and that the discharge can be described by both a Monte Carlo simulation and by a Boltzmann treatment given by Phelps *et al.* (1987).

1. Introduction

The behaviour of electron swarms in gases has been investigated extensively, both experimentally and theoretically, under conditions of low and intermediate swarm energy as measured by the ratio of the applied electric field to the gas number density, E/N . Many practical discharges operate, however, at high E/N (>500 Td). The present project aimed to measure the electron energy distribution function $F(\epsilon)$, in such a discharge and to compare the results with that limited analytical theory which exists. Currently the single and multiple beam models of Phelps *et al.* (1987) are being used. Monte Carlo simulations of these discharges have also been developed.

The direct measurement of the electron energy distribution function (EEDF) by the extraction of electrons through a hole in the discharge cathode and subsequent analysis of these electrons by a retarding potential analyser was attempted by Kenny and Craggs (1970). Losee and Burch (1972) and Makabe *et al.* (1977) also used this technique and published data on the zeroth and first components of the EEDF expansion in spherical harmonics. Such measurements of EEDF have been criticised by Braglia *et al.* (1984) because they are generally performed close to metallic boundaries which may significantly alter the shape of the distribution function at low electron energies. Vrhovac *et al.* (1992) have applied the retarding

* Refereed paper based on a presentation to the Third Japan-Australia Workshop on Gaseous Electronics and Its Applications, held at Yeppoon, Queensland, in July 1994.

potential technique to electrons in argon discharges at moderate and high E/N values. At these elevated swarm energies only a very small proportion of the electron population will be at low energy and hence subject to the gross errors indicated by Braglia *et al.* (1984).

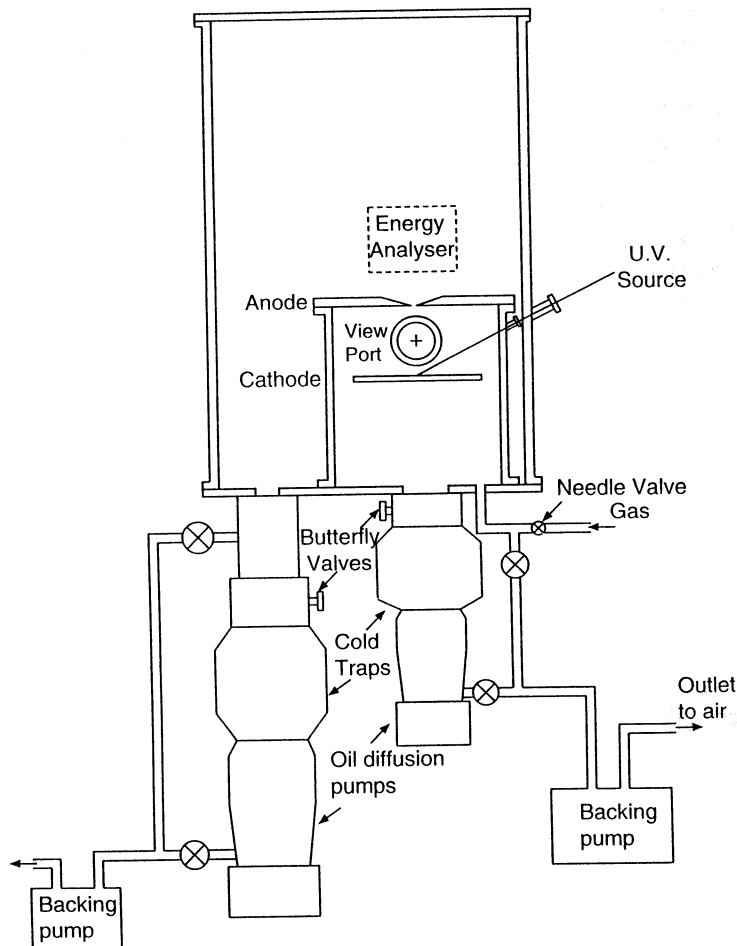


Fig. 1. Schematic of the experimental vacuum system.

2. Experimental Apparatus

A schematic of the vacuum chamber and its contents is shown in Fig. 1. The heart of the apparatus is a cylindrical vacuum vessel 0.8 m in length and with a 0.54 m outside diameter. This vessel was evacuated to a pressure of less than 10^{-5} Pa by means of a 600 ls^{-1} oil diffusion pump backed by a 150 ls^{-1} rotary pump. Heating tapes were used to heat this vessel to about 400 K in order to assist in the outgassing of the metal within the vacuum chamber. Within this outer vessel, mounted on the bottom plate, is the drift cell. The cell consists of a short glass pipe 280 mm in diameter and 175 mm long. The top end plate

doubles as the drift anode. A 200 mm diameter cathode was mounted within the drift cell. The cathode can be repositioned so as to change the electrode separation from zero to 40 mm. The upper plate (the anode) has a 0.5 mm hole in the geometric centre to facilitate the transmission of electrons from the discharge to the outer vacuum chamber.

The drift cell was evacuated to a base pressure of less than 2×10^{-5} Pa by a 150 l s^{-1} oil diffusion pump backed by a three stage rotary backing pump. Gas was admitted to this cell via an MKS model 248A/B automatic control valve which was controlled by an MKS type 250B pressure flow controller. An MKS type 127A capacitance manometer was used to measure the gas pressure with a sensitivity of 0.1 Pa in a pressure range of 1.00 to 250 Pa. The electron egress hole in the anode constitutes a gas loss for which the gas control system has to allow. With the above system the gas pressure within the drift cell could be maintained constant to within 0.1% over the range of pressures used.

The drift tube anode is 25 mm thick which enables the egress hole to be tapered from the outer surface, so giving a 0.5 mm diameter with a 0.2 mm thick knife-edge. The diameter and the thickness of the hole have to be such that there is a very small probability of an electron undergoing a collision in the gas or at the walls while passing through the hole, i.e. effusive flow. This demands that the electron mean free path is large compared with the hole diameter, i.e. $(NQ)^{-1} < 5 \times 10^{-4}$ m. At low values of E/N the drift gap operated below the breakdown potential and hence a steady voltage could be applied to the drift gap. At higher E/N , however, the necessary voltage was above breakdown. In these latter cases the voltage was applied only for a short time during which the electronic counting gate was open. This prevented the current growing sufficiently to swamp the electron counting circuits. The voltage pulse was applied for between 0.5 and 12 μs with a repetition rate of between 50 Hz and 140 kHz. The voltage pulser, made in these laboratories, is capable of maintaining a constant negative voltage on the cathode for the full period that it is applied and for which the counting electronics are gated open.

Both types of electron energy analyser discussed below require a ramped voltage to scan the electron energy range. This was obtained from a voltage ramp power supply designed and built in these laboratories. The pulser also supplies the start signal to the computer MCA system.

A schematic diagram of the electrical components used for steady state pre-breakdown discharges is shown in Fig. 2. The electron source is an indirectly heated oxide cathode mounted behind a 0.5 mm hole in the cathode. The drift chamber anode is grounded and the cathode maintained at a negative voltage of up to 2 kV.

Use of only pre-breakdown discharges would have severely limited the range of E/N that could be investigated. Also it is of interest to investigate the mechanisms of the discharge at and after breakdown. Consequently, discharge conditions ranging from just below to just above V_s (trans-breakdown) and well above V_s (post-breakdown) were studied. In the case of the trans-breakdown discharges the oxide cathode was found to provide too high an initial electron flux which after amplification at these high E/N values swamped the electron counting circuits. Hence a 100 W mercury arc lamp mounted externally to the chamber was used to provide ultra-violet radiation which was admitted to the

drift chamber via a quartz window and was incident upon the cathode at grazing incidence. Again the anode is earthed and a negative high tension is applied to the cathode.

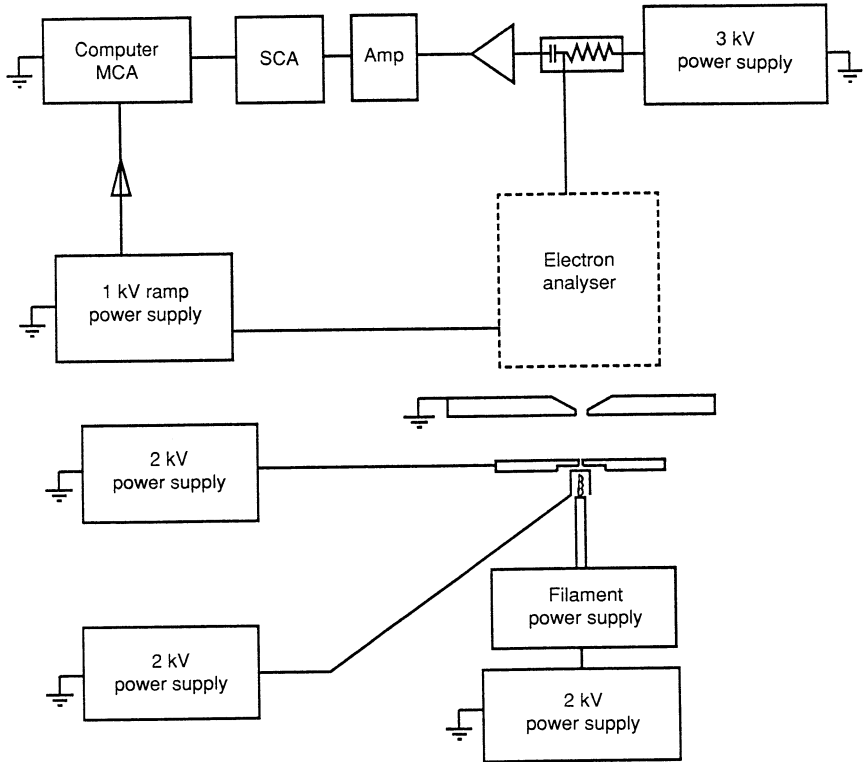


Fig. 2. Schematic of the electrical arrangement used for pre-breakdown measurements. Post-breakdown measurements use similar electronics except that the electrons are initiated by the incidence of ultra-violet radiation on the cathode.

The retarding field analyser has a parallel plate geometry which allows its placement above the anode aperture. Electrons entering the analyser are retarded by the electrostatic field produced by stainless steel mesh plates consisting of a ring with an inner diameter of 500 mm and an outer diameter of 120 mm. The plates are 1 mm in thickness. The retarding plates are placed one above the other with the ramp voltage applied to the upper plate and the lower plate grounded to earth (the same potential as the anode). If the kinetic energy of the electrons entering the analyser is $E = eV > V_0$, the voltage applied to the retarding grid, they reach the electron multiplier and are counted, and if $V_0 < V_i$ they will be repelled. This analyser has several disadvantages due to a limited resolution and difficulties in extracting the EEDF from the raw data. In this case the raw data are not the number of electrons with a certain energy $N(\epsilon)$, but the number of electrons with energy higher than the selected value, viz. the integral of $N(\epsilon)$. This latter must thus be differentiated to give the required EEDF. Low level noise in $\int N(\epsilon)$ versus ϵ is amplified by the differentiation so introducing added uncertainties. The cylindrical mirror analyser was chosen for its lower

degradation in resolution over a large energy range with second order focussing easily obtainable (Risley 1972). The cylindrical mirror analyser was designed using the parameters of Risley (1972) with a total distance from the source and the image to the inner cylinder of 2 cm. This choice produced a relatively small spectrometer 90 mm in length with inner and outer radii of 10 and 37.05 mm respectively. The spectrometer consists of a section of two concentric cylinders of machined aluminium capped by end and side plates constructed of 3 mm printed circuit board. Potentials are applied to the side and end plates to produce equipotential surfaces associated with the radial electric field inside.

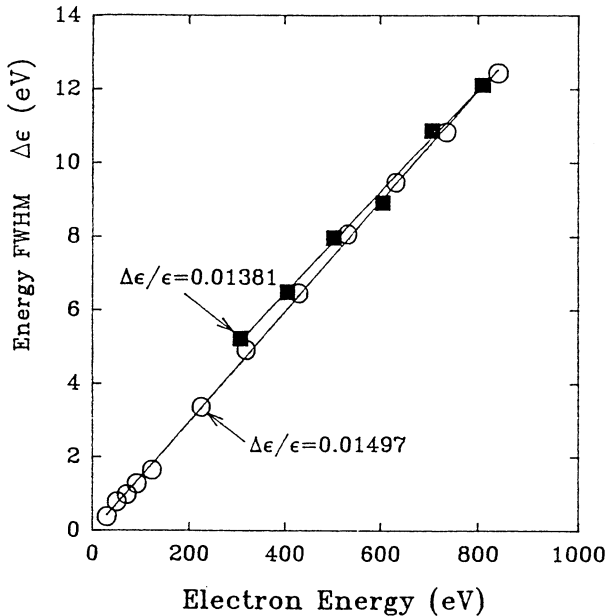


Fig. 3. FWHM values $\Delta\epsilon$ as a function of electron energy ϵ for both the parallel plate retarding potential analyser (squares) and the electrostatic cylindrical analyser (circles).

The ramp voltage was applied to the top plate which is connected to the grounded bottom plate via a series of 220 k Ω resistors. Electrons with a kinetic energy corresponding to the applied voltage on the top plate were collected by the channel electron multiplier. Both analysers have all conducting surfaces coated with graphite to minimise electron reflection and secondary emissions. The resolution $\Delta\epsilon$ at the full-width half-maximum (FWHM) of both analysers was measured by allowing electrons to cross the drift gap in vacuum, so obtaining the full gap energy, and then to enter the spectrometers in both the pulsed and steady stream set-ups. Fig. 3 shows that both types of analyser demonstrate a similar resolution and that the resolution is good enough for details within the electron energy spectrum spread over a few eV to be obvious. Irrespective of the type of discharge studied the electron output from the energy analyser is directed into a Mullard-type 8318BL channel electron multiplier. The signal from this detector is then recorded and stored by a computer based MCA running Canberra Accuspec MCA software.

3. Results

Data on the electron flux as a function of electron energy were obtained using both the parallel plate analyser and the cylindrical mirror analyser over the range $300 < E/N < 2500$ Td using a gas pressure range of $6 < p < 250$ Pa. A Paschen curve (breakdown potential as a function of the product of the gas pressure and electrode separation) for neon was obtained. This is shown in Fig. 4 which includes the experimental data points indicating those which are pre-breakdown and those in the post-breakdown regime. Data taken at E/N values below breakdown were taken mostly using a steady state discharge, whilst discharges at values of E/N corresponding to trans-breakdown and post-breakdown discharges were studied predominantly in pulsed discharges.

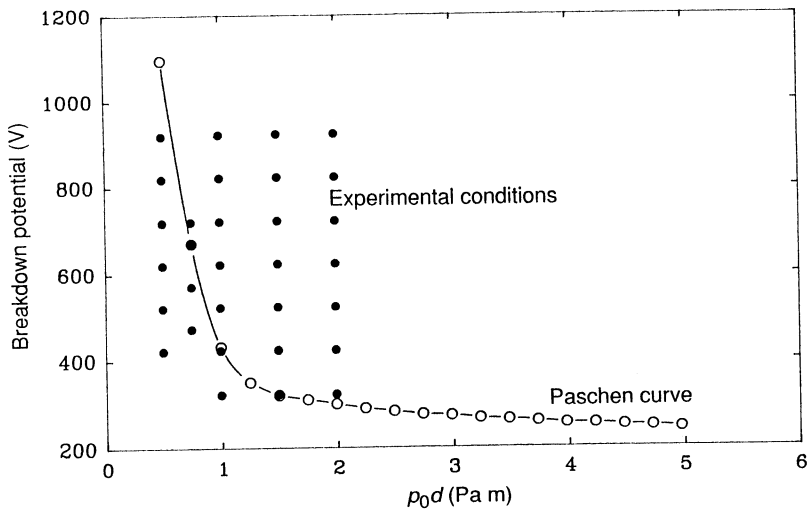


Fig. 4. Graph of the breakdown potential V_s (open circles) as a function of the product of the gas pressure (at 273 K) and the drift gap separation p_0z . Solid circles represent the array of experimental conditions used in the investigation.

It was necessary to ensure that both types of analyser gave the same results for identical discharges. Fig. 5 shows data from each analyser at $E/N = 2300$ Td. It may be seen that there is no difference in the data taken using either a steady or a pulsed discharge. In both cases the electron number density does not go to zero as the electron energy goes to zero. It is believed that this is due to the emission of secondary electrons from the anode resulting from the impact of high energy electrons. These electrons will be attracted back to the anode but will produce a large flux of low energy electrons, some of which will pass through the analysis hole into the analyser (Kelly 1990; Kelly and Blevin 1989). A similar effect is seen with the electrostatic mirror spectrometer as shown below.

We intend to treat all experimental data with a similar theoretical analysis. For this to be reasonable all data from both pre- and post-breakdown discharges must be of the same functional form—if the process of breakdown changes the nature of the discharge any comparison will not be valid. Hence at $pd = 153$ Pa m data were compared at $E/N = 1000, 1250$ and 2000 Td. This is shown in

Fig. 6. It is immediately evident that there are three quite discrete populations of electrons which may be classified as the swarm electrons, the runaway electrons and the beam electrons. The first are electrons which have experienced many electron-atom collisions. These are expected to be similar to the electron swarms

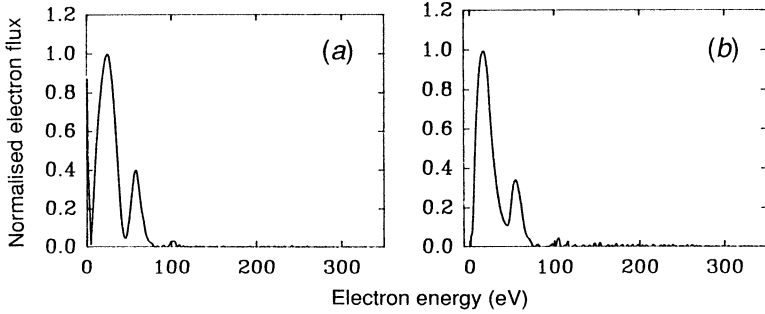


Fig. 5. Experimental electron energy distribution at $E/N = 2280$ Td, $p_0 = 13.3$ Pa and $d = 4$ cm for (a) a parallel plate analyser and (b) an electrostatic cylindrical analyser.

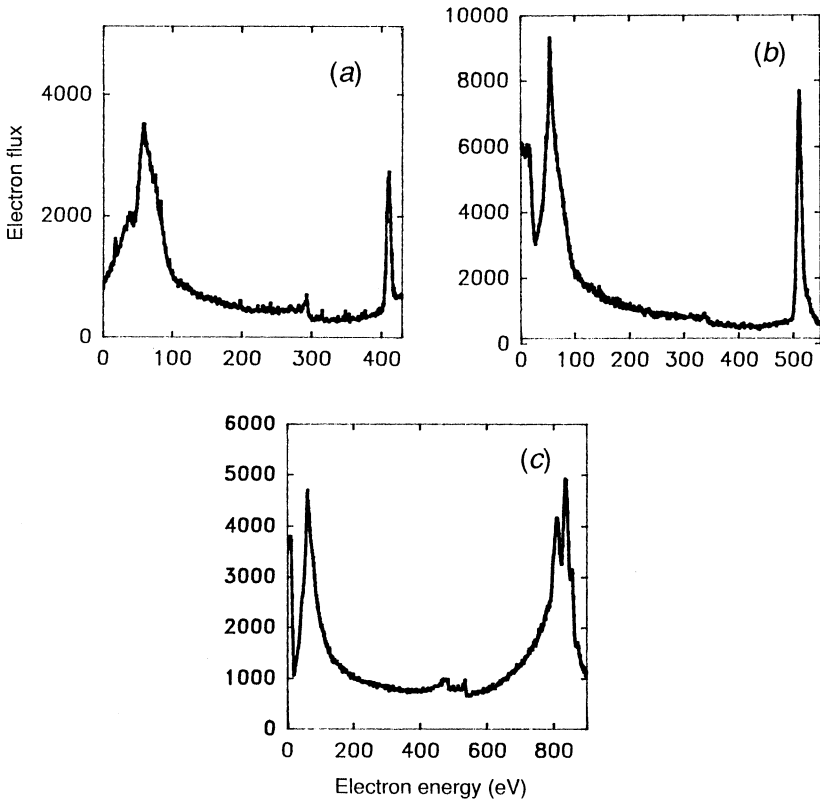


Fig. 6. Experimental electron energy distribution in neon at $p_0 d = 0.947$ Pa m taken using the cylindrical analyser. The breakdown potential at this pd is 500 V: (a) at an applied voltage of 400 V, i.e. below V_s ; (b) at a voltage of 500 V, i.e. at breakdown; and (c) at a voltage of 800V, i.e. well above V_s .

in low energy discharges and hence the transport parameters of these electrons should not be position dependent. The runaway electrons start as swarm electrons with energies in the high energy tail of the electron energy distribution. At these higher energies the cross section for collision reduces and hence the higher the energy that these electrons achieve the less likely they are to have collisions. The electrons thus run away from the main swarm and contribute to the observed population. The transport properties of this sub population will be expected to be position dependent. The final group of electrons are the beam electrons which have undergone either no collisions or, at most, only two or three from the time the electrons left the cathode. Again the properties of this group will be spatially dependent.

4. Data Analysis

The theoretical modelling of these highly non-equilibrium discharges is vital to the interpretation and understanding of experimental data. A Monte Carlo approach has been adopted due to its flexibility for modelling discharges which are both under 'equilibrium' conditions and those that have extensive non-equilibrium regions. The Monte Carlo simulation technique also allows the details of electron interaction at the electrode boundaries to be considered, as described by Kelly (1990) and Kelly and Blevin (1989). The development of the simulation technique has been discussed by both Segur *et al.* (1983) and Hunter and Christophorou (1984). The Monte Carlo technique is a very powerful method and provides all phase space information for electrons in the gas which can be used to directly obtain transport parameters or obtain the electron energy distribution function $F(\epsilon)$ throughout the discharge region. The Monte Carlo code used in this work is based upon the 'null collision' technique introduced by Skullerud (1968) and developed in the present form by Brennan (1986) and Brennan *et al.* (1990). The essential information required for a Monte Carlo simulation is a full set of cross-section data. A comprehensive set of inelastic excitation cross sections for 24 levels in neon has been published by Puech and Mizzi (1991). The ionisation cross sections of Krishnakumar and Srivastara (1988) were used for the production of Ne^+ , Ne^{2+} and Ne^{3+} by electron collision. Before the simulation was applied to high E/N discharges the method and cross-section set was used to predict transport parameters at low E/N as a test of the accuracy of the programme. These predictions are shown in Fig. 7 where the present work is compared with previous theoretical and experimental data. The excellent agreement seen in Fig. 7 supports the use of the simulation at high E/N . Fig. 8 shows experimental data on the swarm mean electron energy as a function of E/N compared with the predictions of the Monte Carlo simulation. Again the agreement is excellent.

Phelps *et al.* (1987) used a moment solution of the one-dimensional electron Boltzmann equation. These authors used both energy and momentum balance conditions to obtain relationships between the value of E/N and the distance an electron must move within the discharge in order to come into equilibrium with the field and electron-molecule collisions. They considered both a 'single beam' model (no cathode secondary emission) and a 'multibeam' model in which each cathode secondary instigates a beam. Fig. 9 represents the various transitions as a curve of 'effective distance' Nz against E/N . The sloping straight lines represent

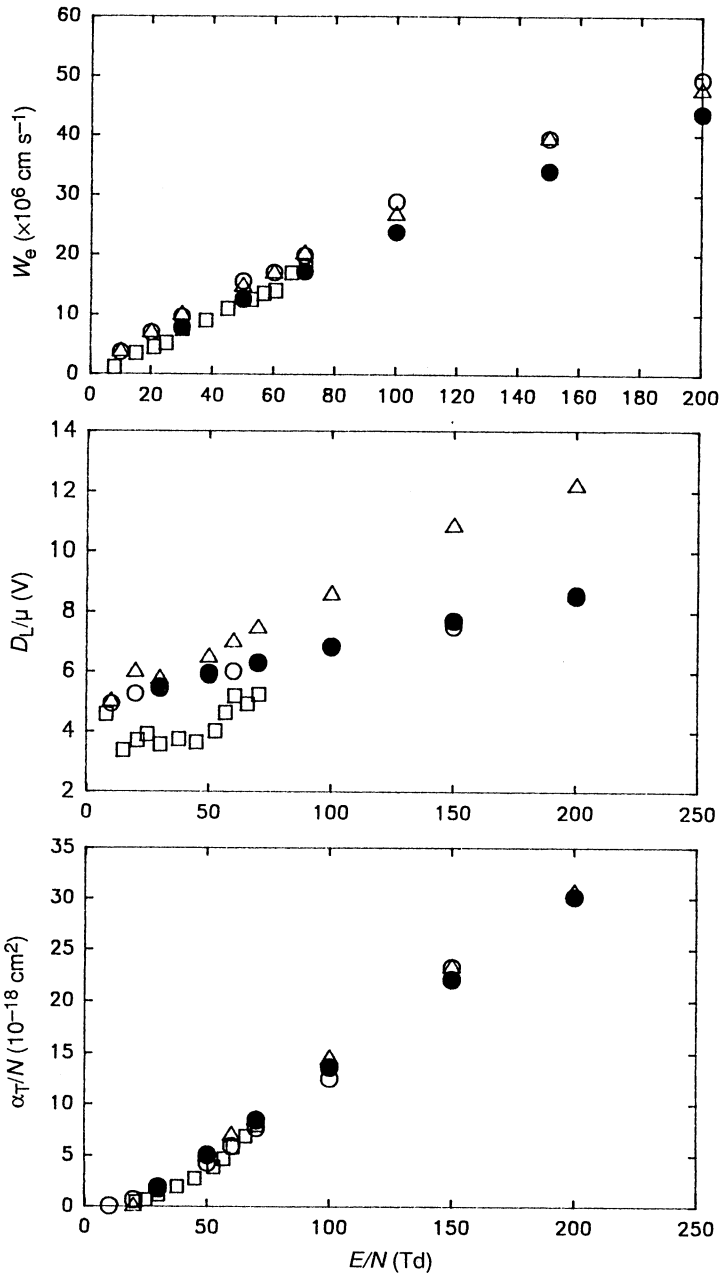


Fig. 7. The electron drift velocity, the ratio of the longitudinal diffusion coefficient to mobility and the ionisation coefficient for neon as a function of E/N : solid circles, present Monte Carlo simulation results; open circles, Puech and Mizzi (1991); squares, Dall'Armi *et al.* (1992); and triangles, Kükükarpaci *et al.* (1981).

the energy that an electron would acquire in the effective distance Nz under the influence of the electric field in the absence of collisions, i.e. 'free fall'. Included in this graph are the boundary conditions between free fall and drift motion as indicated by the energy balance and the momentum balance approaches. Also

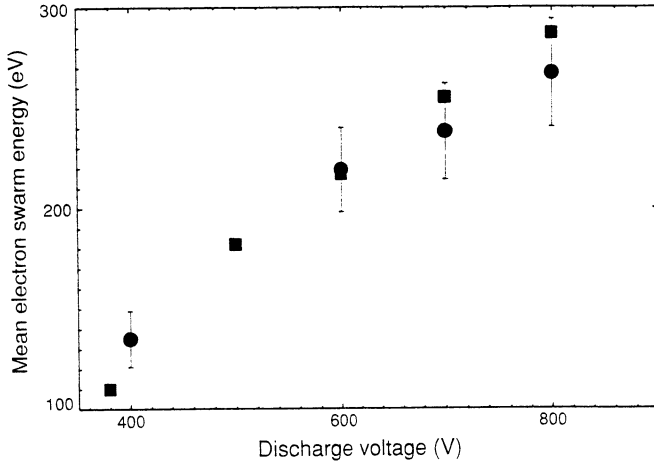


Fig. 8. Mean electron energy ϵ as a function of E/N : circles, experimental data; squares, Monte Carlo simulation.

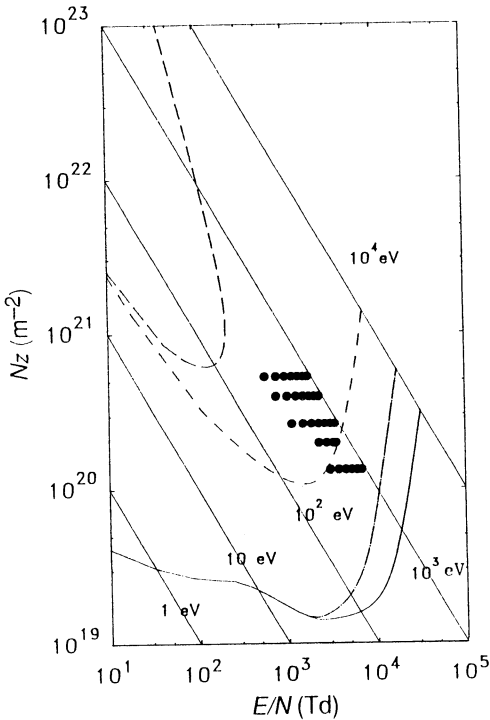


Fig. 9. Effective drift gap Nz as a function of E/N in neon calculated from the theory given by Phelps *et al.* (1987). The cross sections of Puech and Mizzi (1991) were used: solid curve, multibeam energy balance; long-dash curve, single beam energy balance; short-dash curve, multibeam momentum balance; dash-dot curve, single beam momentum balance; and solid circles, experimental points.

shown are the experimental points at which data have currently been obtained and which can be seen to straddle the single beam energy balance equation. If the data point is below the relaxation limit, runaway and beam electrons will be evident in the experimental data. Above the limit equilibrium swarm electrons should be observed. Examination of the raw data shows that runaway and beam

electrons do not exist when the experimental conditions are below the curve, but do appear when the experimental conditions are above this line.

5. Conclusion

The present work has demonstrated that the present techniques will yield reliable and meaningful data on the electron energy distribution, not only in pre-breakdown discharges, but over a much wider E/N range into the post-breakdown regime. The data so obtained are in agreement with both a Monte Carlo simulation of a discharge in neon and also with the Boltzmann equation treatment of Phelps *et al.* (1987). The present indications are that in the latter work the single beam energy balance equation adequately predicts the electron swarm behaviour.

References

- Braglia, G. L., Romano L., and Diligenti, M. (1984). *Nuovo Cimento* **79**, B93.
- Brennan, M. J. (1986). Ph.D. Thesis, Flinders University.
- Brennan, M. J., Garvie, A. M., and Kelly, L. J. (1990). *Aust. J. Phys.* **43**, 27–43.
- Dall'Armi, G., Brown, K. L., Purdie, P. H., and Fletcher, J. (1992). *Aust. J. Phys.* **45**, 185.
- Hunter, S. R., and Christophorou, L. G. (1984). 'Electron-Molecule Interactions and Their Applications', Vol. 2 (Ed. L. G. Christophorou), p. 90 (Academic: Orlando, Fla.).
- Kelly, L. J. (1990). Ph.D. Thesis, Flinders University.
- Kelly, L. J., and Blevin, H. A. (1989). 19th Int. Conf. on Phenomena in Ionised Gases, Belgrade, Vol. 4, p. 892.
- Kenny, T. E., and Craggs, J. D. (1970). *J. Phys. B* **3**, 251.
- Krishnakumar, E., and Srivastara, S. K. (1988). *J. Phys. B* **21**, 1055.
- Kucukarpaci, H. N., Saelee, H. T., and Lucas, J. (1981). *J. Phys. D* **14**, 9.
- Losee, J. R., and Burch, D. S. (1972). *Phys. Rev. A* **6**, 1652.
- Makabe, T., Goto T., and Mori, T. (1977). *J. Phys. B* **10**, 1781.
- Phelps, A. V., Jelenkovic, B. M., and Pitchford, L. C. (1987). *Phys. Rev. A* **36**, 5327.
- Puech, V., and Mizzi, S. (1991). *J. Phys. D* **24**, 1974.
- Risley, J. S. (1972). *Rev. Scient. Instrum.* **43**, 95.
- Segur, P., Yousfi, M., Boeuf, J. P., Marode, E., Davies, A. J., and Evans, J. G. (1983). In 'Electric Breakdown and Discharges in Gases' (Eds E. E. Kunhardt and L. H. Luessen), NATO ASI Series B; Vol. 89A, p. 331 (Plenum: New York).
- Skullerud, H. R. (1968). *J. Phys. D* **1**, 1567.
- Vrhovac, S. B., Radovanov, S. B., Petrovic, Z. Lj., and Jelenkovic, B. M. (1992). *J. Phys. D* **25**, 217–25.

